Deformation Behavior and Microstructure Evolution of the Cu-2Ni-0.5Si-0.15Ag Alloy During Hot Compression

YI ZHANG, ALEX A. VOLINSKY, QIAN-QIAN XU, ZHE CHAI, BAOHONG TIAN, PING LIU, and HAI T. TRAN

Hot deformation behavior of the Cu-2Ni-0.5Si-0.15Ag alloy was investigated by hot compression tests using the Gleeble-1500D thermo-simulator in the 873 K to 1073 K (600 °C to 800 °C) temperatures range with the 0.01 to 5 s^{-1} strain rate. The flow stress strongly depends on the deformation parameters, including temperature and strain rate. The flow stress decreases with the deformation temperature and increases with the strain rate. The constitutive relationship between the peak stress, the strain rate, and the deformation temperature can be described by the Zener–Hollomon Z parameter in the hyperbolic sine function with the hot deformation activation energy of 316 kJ/mol. The dynamic recrystallization (DRX) is one of the important softening mechanisms of the Cu-2Ni-0.5Si-0.15Ag alloy during hot deformation. The DRX behavior of the Cu-2Ni-0.5Si-0.15Ag alloy is strongly affected by the Z parameter. Lower Z parameter leads to more adequate DRX proceeding.

I. INTRODUCTION

THE lead frame is the foundation of the integrated circuits, which plays the main role of supporting the chip, along with electrical signal transmission and heat dissipation in the integrated circuit. Thus, the lead frame is very important for the microelectronics industry.[1] The lead frame material should be adequate heat and electrical conductor, have high strength and heat resistance, along with excellent processing properties. Many experts have conducted a lot of research to obtain the desired material for the lead frame. Due to the high electrical conductivity, Cu alloys are widely used as the lead frame materials, including Cu-Ni-Si, Cu-Fe, Cu-Fe-P, Cu-Cr-Zr, and Cu-Ag alloys. Among these alloys, Cu-Ni-Si has become a research focus due to its high strength and hardness, good processing properties, and modest electrical conductivity.[2–13]

Cu-Ni-Si alloy is one of the age-hardening alloys. Corson had been the first to find the hardening behavior of this alloy in 1927, and attributed this age-hardening behavior to the precipitation of the δ-Ni_2Si phase.[14] The microalloyed technology has been used to further improve the comprehensive performance of the Cu-Ni-Si alloy, and then the Cu-Ni-Si-Ag alloy was developed. The strength and hardness of the Cu-Ni-Si alloy can be enhanced significantly by adding a small quantity of silver. Silver atoms dissolve in the matrix and induce obvious hardening. Solid solution strengthening tends to decrease the electrical conductivity of the Cu alloys, since lattice distortions induced by the solute atoms increase electron scattering.[15,16] However, the solid solution of Ag atoms does not cause a clear decline in the electrical conductivity of the Cu-Ni-Si alloy, since Ag addition promotes Ni_2Si phase precipitation. The Ni_2Si phase precipitation weakens the lattice distortion, which is induced by the Ni and Si atoms, so it can be said that the precipitation of the Ni_2Si phase offsets the adverse effects of Ag addition on the electrical conductivity. There are many similar results of Ag affecting precipitation of copper alloys.[17,18] In the previous study, it was found that the comprehensive performance of the Cu-2Ni-0.5Si alloy can be improved by the addition of 0.15 wt pct Ag, and the hardness, electrical conductivity, and strength of the Cu-2Ni-0.5Si-0.15Ag alloy increased by 2.1, 15.3, and 8.7 pct, respectively, compared with the Cu-2Ni-0.5Si alloy.[19]

Because of the excellent comprehensive properties, the Cu-2Ni-0.5Si-0.15Ag alloy has a great prospect for applications in the microelectronics industry as the lead frame material. Hot rolling is commonly used to manufacture the lead frame strips, thus studying hot deformation behavior and deformation resistance is quite useful for producing the Cu-2Ni-0.5Si-0.15Ag alloy strips. Studies show that hot deformation parameters, such as temperature and strain rate, have a major influence on the hot deformation behavior of metals. It is necessary to study the constitutive relation of the

YI ZHANG, Associate Professor, is with the School of Materials Science and Engineering, Henan University of Science and Technology, Luoyang 471003, China and also Visiting Professor in the Department of Mechanical Engineering, University of South Florida, Tampa 33620. Contact e-mail: zhshgu436@163.com ALEX A. VOLINSKY, Associate Professor, and HAI T. TRAN, Ph.D. Graduate Student, are with the Department of Mechanical Engineering, University of South Florida. Conatct e-mail: volinsky@usf.edu QIAN-QIAN XU and ZHE CHAI, Ph.D. Graduate Students, and BAOHONG TIAN, Professor, are with the School of Materials Science and Engineering, Henan University of Science and Technology.

Cu-2Ni-0.5Si-0.15Ag alloy in order to optimize the hot rolling process.

In this study, the effects of deformation parameters, including temperature and strain rate, on the flow stress of the Cu-2Ni-0.5Si-0.15Ag alloy have been investigated by hot compression tests. The constitutive constants of this alloy have been determined, and constitutive equations relating the Zener–Hollomon Z parameter and hot deformation activation energy, Q, have been derived for this alloy. The effects of deformation parameters on the microstructure evolution of this alloy during hot deformation have been also studied in detail. This study provides valuable information for optimizing the hot deformation processing parameters of the lead frame strips with desirable microstructure.

II. EXPERIMENTAL PROCEDURE

The experimental alloy was melted in a vacuum induction furnace under argon atmosphere, using cathode copper, pure nickel, and pure silver, and then cast into a low-carbon steel mold with $\Phi 83$ mm $\times$ 150 mm dimensions. The alloy chemical composition is as follows in wt pct: 1.96Ni, 0.51Si, 0.15Ag, and Cu balance. The chemical composition of the alloy was determined by the SPECTRO ARCOS ICP-OES analyzer. The ingot was homogenized at 1203 K (930 °C) for 2 hour to remove the alloying elements segregation and then forged into bars with 25-mm diameter. Finally, the forged bars were solution treated at 1173 K (900 °C) for 1 hour, followed by water quenching.

Cylindrical compression specimens with 10-mm diameter and 15-mm height were machined from the solution-treated bars. Figure 1 shows the microstructure of the Cu-2Ni-0.5Si-0.15Ag alloy after solution treatment. Hot compression tests were carried out using the Gleeble-1500D thermo-simulator at a strain rate of 0.01 to 5 s^{-1} and deformation temperature of 873 K to 1073 K (600 °C to 800 °C). The specimens were heated to the deformation temperature at 10 K/s (10 °C/s) rate. Before deformation, all specimens were kept at deformation temperature for 180 s to make sure that the temperature is homogeneous. All specimens were compressed to a true strain of 0.9. After compression testing, the specimens were immediately quenched in water. The deformed specimens were sectioned through the longitudinal axis. All specimens were polished and then etched with a solution of FeCl$_3$ (5 g) + C$_2$H$_5$OH (85 mL) + HCl (10 mL). The microstructure was observed using optical microscopy (OLYMPUS PMG3).

III. RESULTS AND DISCUSSION

A. Flow Stress Behavior

The true stress–strain curves of the Cu-2Ni-0.5-Si-0.15Ag alloy deformed at various strain rates and deformation temperatures are shown in Figure 2. The flow stress level increases with increasing the strain rate
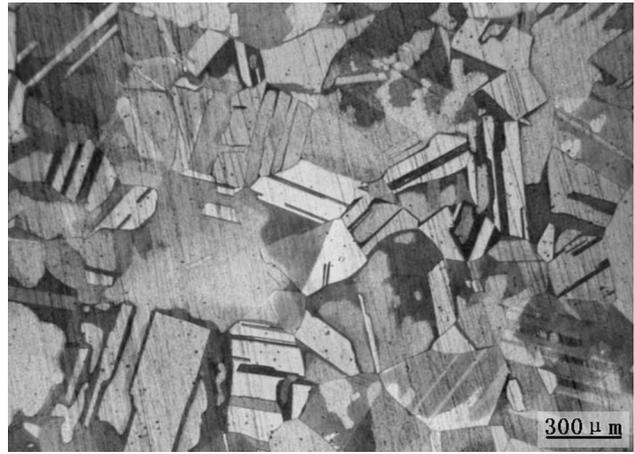

Fig. 1— Microstructures of the Cu-Ni-Si-Ag alloy after solution treatment at 1173 K (900 °C) for 1 h.

and decreasing the deformation temperature. For the same strain rate and higher deformation temperature, the flow stress level is lower. It can be seen from Figure 2(a) that during the compression test at 873 K (600 °C) and 0.01 s^{-1}, continuous strain hardening was observed over the entire deformation range. However, the strain hardening behavior does not appear in other stress–strain curves, even at higher strain rates. As mentioned, the Cu-2Ni-0.5Si-0.15Ag alloy is age-hardened copper alloy, and its aging treatment is performed at around 773 K (500 °C). Therefore, when the specimen is deformed at 873 K (600 °C), the Ni$_2$Si phase precipitates out during deformation, leading to a monotonous increase of the flow stress. Moreover, the Ni$_2$Si phase nucleation needs time, so the strain hardening behavior can only be observed during the hot deformation with a low strain rate. On the other hand, the other stress–strain curves exhibit flow softening, as seen in Figure 2(c). The flow softening behavior of the metallic materials during hot deformation is due to the dynamic recovery (DRV) and dynamic recrystallization (DRX). The flow stress curves with the DRV feature first reach the maximum stress, followed by a steady flow stress. For example, the flow curve of the sample deformed at 873 K (600 °C) and 1 s^{-1} belongs to this type (Figure 2(c)). The flow stress curves with the DRX feature exhibit a peak stress, after which the flow stress decreased gradually until the end of compression, showing dynamic softening. For example, the flow curve of the sample deformed at 1023 K (750 °C) and 1 s^{-1} belongs to this type in Figure 2(c).

B. Constitutive Analysis

For the hot deformation of metals, the constitutive relationship between the flow stress, strain rate, and deformation temperature can be expressed using the following equations[20–22]:

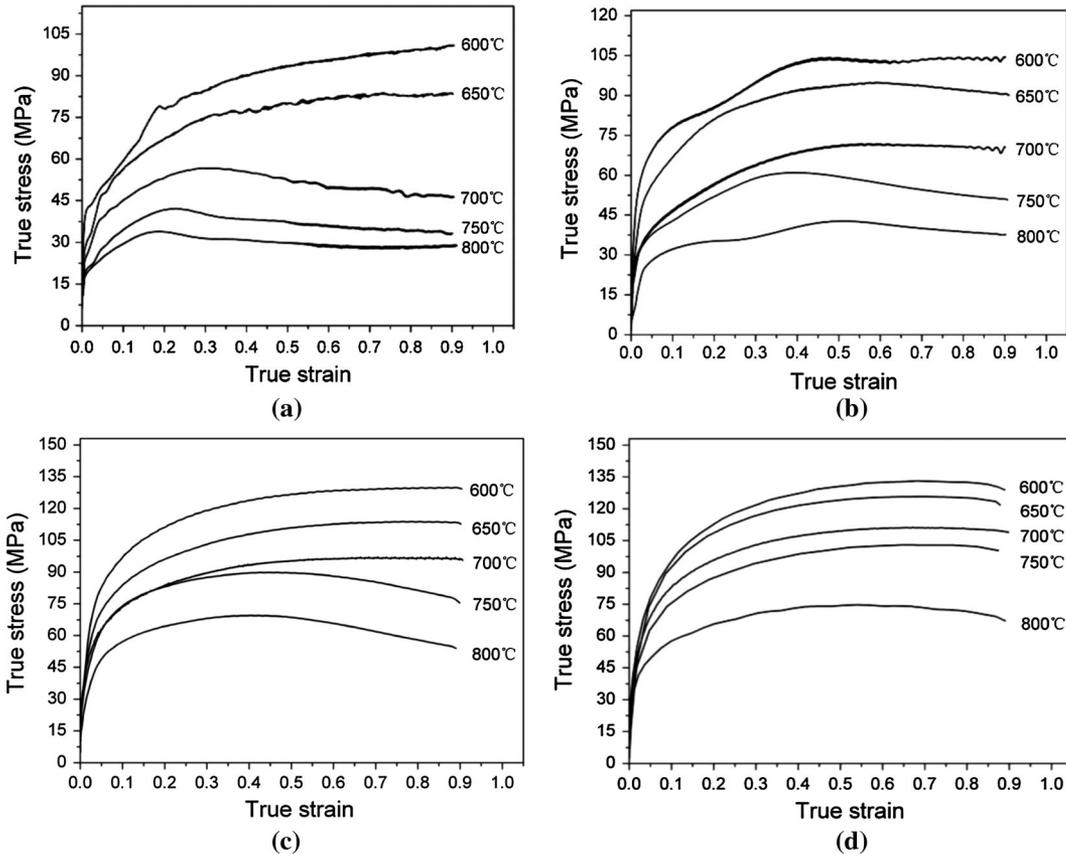$$\dot{\varepsilon} = A_1 \sigma^n \exp\left(-\frac{Q}{RT}\right) \ (\alpha\sigma < 0.8), \qquad [1]$$

Fig. 2— True stress–true strain curves of the Cu-Ni-Si-Ag alloy during hot compression at various temperatures and different strain rates of: (a) 0.01 s^{-1}; (b) 0.1 s^{-1}; (c) 1 s^{-1} and (d) 5 s^{-1}.

$$\dot{\varepsilon} = A_2 \exp(\beta\sigma) \exp\left(-\frac{Q}{RT}\right) \ (\alpha\sigma > 1.2), \qquad [2]$$

$$\dot{\varepsilon} = A[\sinh(\alpha\sigma)]^n \exp\left(-\frac{Q}{RT}\right), \qquad [3]$$

where $\dot{\varepsilon}$ is the strain rate, T is the absolute temperature, σ is the flow stress, R is the gas constant, Q is the activation energy for hot deformation and A, A_1, A_2, n, n_1, α, and β are material constants. The power law in Eq. [1] breaks down at high stress levels, whereas the exponential law in Eq. [2] breaks down at the low stress levels. The hyperbolic sine law in Eq. [3] is a universal form suitable for a wide stress range.

Hot deformation behavior of metallic materials is represented by the Zener–Hollomon parameter (Z), which is related to the strain rate, deformation temperature, and hot deformation activation energy as

$$Z = \dot{\varepsilon} \exp\left(\frac{Q}{RT}\right). \qquad [4]$$

By combining Eqs. [3] and [4], the relationship between the Z parameter and the flow stress can be described by the following equation:

$$Z = A[\sinh(\alpha\sigma)]^n. \qquad [5]$$

In this paper, the peak stress, σ_p, is used for the σ term in the above equations. The stress multiplier, α, is an adjustable constant that brings the $\alpha\sigma_p$ values into a suitable range, and α is defined as in[23–25]:

$$\alpha = \frac{\beta}{n} \approx \frac{\beta}{n_1}. \qquad [6]$$

The stress exponent, n_1, in the power law determined from the experimental data measured at high temperatures and low strain rates, whereas β in the exponential law determined from the experimental data measured at low temperatures and high strain rates. Finally, the values of n_1 and β were determined as 6.14 and 0.124, respectively, and then the stress multiplier, α, was determined as 0.02.

By taking natural logarithms and then partial derivatives of both side of Eq. [3], one gets

$$\ln\dot{\varepsilon} = \ln A + n\ln[\sinh(\alpha\sigma)] - \frac{Q}{RT} \qquad [7]$$

$$\partial(\ln\dot{\varepsilon}) = n\partial[\ln\sinh(\alpha\sigma)] - \frac{Q}{R}\partial\left(\frac{1}{T}\right). \qquad [8]$$
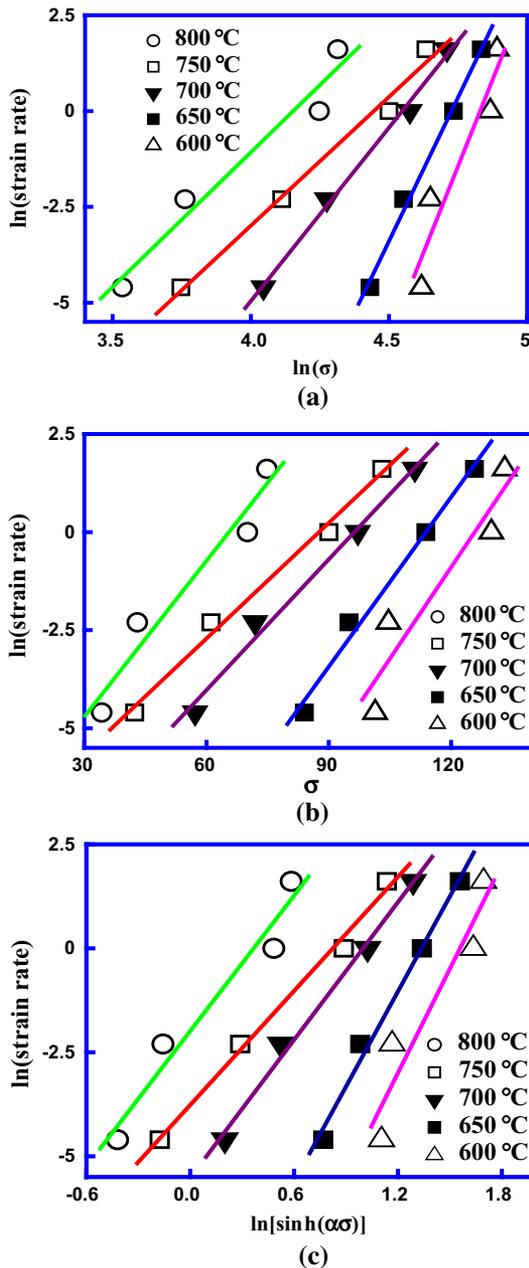
Fig. 3— Peak stress *vs* strain rate at different deforming temperatures, based on the three semi-empirical models: (*a*) the power law model; (*b*) the exponential law model; and (*c*) the hyperbolic sine model.
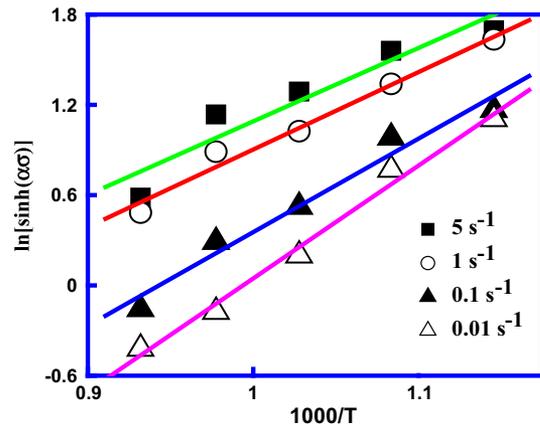

Fig. 4— Variation of $\ln[\sinh(\alpha\sigma)]$ *vs* $(1000/T)$ at different strain rates for evaluating the hot deformation activation energy, Q.

If T is a constant, Eq. [8] can be written as

$$n = \frac{\partial(\ln\dot{\varepsilon})}{\partial\ln[\sinh(\alpha\sigma)]}\Big|_T. \qquad [9]$$

If $\dot{\varepsilon}$ is a constant, Eq. [8] can be written as

$$Q = R\left[\frac{\partial(\ln\dot{\varepsilon})}{\partial\ln[\sinh(\alpha\sigma)]}\right]_T \left[\frac{\partial\ln[\sinh(\alpha\sigma)]}{\partial(1/T)}\right]_{\dot{\varepsilon}} = RnS. \qquad [10]$$

Here, n and S are the slopes of the plots of $\ln\dot{\varepsilon}$ *vs* $\ln[\sinh(\alpha\sigma)]$ at constant temperature and $\ln[\sinh(\alpha\sigma)]$ *vs* $1000/T$ at constant strain rates, respectively. A good linear relationship between $\ln\dot{\varepsilon}$ and $\ln\sigma$, $\ln\dot{\varepsilon}$ and σ, $\ln\dot{\varepsilon}$ and $\ln[\sinh(\alpha\sigma)]$ exists when T remains constant, as seen in Figure 3(a), (b) and (c), respectively. It was shown that the $\ln[\sinh(\alpha\sigma)]$ is linear with $(1000/T)$ when $\dot{\varepsilon}$ remains constant in Figure 4. Then the values of n and S can be determined as 5.86 and 6.50, respectively, by means of linear regression analysis. Consequently, the value of Q for the experimental alloy is 316.4 kJ/mol. The hot deformation activation energy Q is an important physical parameter serving as an indicator of the degree of deformation difficulty in plastic deformation. The hot deformation activation energy Q for the Cu-2Ni-0.5Si-0.15Ag alloy is higher than for the KFC[TM] copper alloy, but lower than for the Cu-3.45 wt pct Ti alloy. The value of Q for the Cu-2Ni-0.5Si-0.15Ag alloy is close to that of the C194 alloy with the following chemical composition in wt pct: 2.43Fe, 0.02P, and 0.13Zn. The higher Q value for the Cu-2Ni-0.5Si-0.15Ag alloy may be associated with the additions of Ni and Ag atoms, which act as extra obstacles for dislocations motion, and increase the flow stress level during hot deformation. In addition, the Ag addition promotes the Ni_2Si phase precipitation, while the dynamic precipitation of the Ni_2Si phase may also increase the flow stress. Generally, the value of Q is a function of the chemical composition of the alloy and increases with the alloying elements content.

In order to determine the value of A, Eq. [5] can be rewritten as

$$\ln Z = \ln A + n\ln[\sinh(\alpha\sigma)]. \qquad [11]$$

It can be found that $\ln A$ is the intercept of the plots of $\ln Z$ *vs* $\ln[\sinh(\alpha\sigma)]$. The relationship between $\ln[\sinh(\alpha\sigma)]$ and $\ln Z$ is plotted in Figure 5. It can be seen that there is a linear relationship between $\ln[\sinh(\alpha\sigma)]$ and $\ln Z$, and the linear correlation coefficient is above 0.97. Thus, the
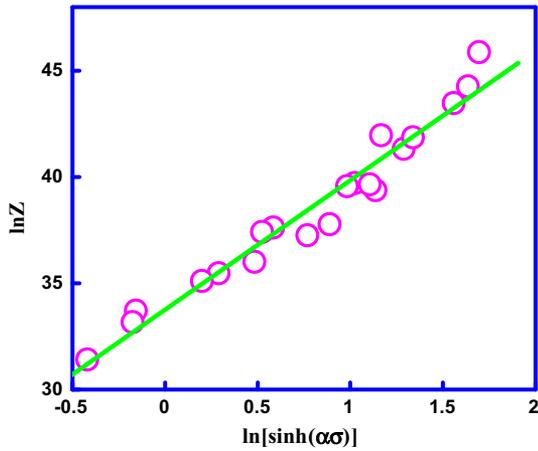
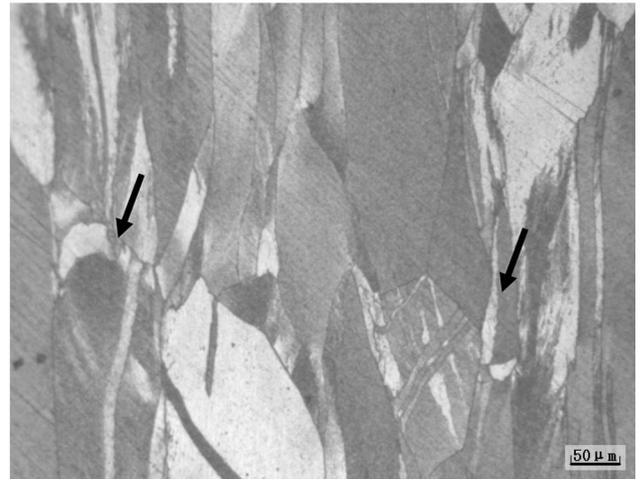Fig. 5— The Zener–Hollomon parameter, *Z*, as a function of the flow stress.

constitutive equation of the Cu-2.0Ni-0.5Si-0.15Ag alloy in the hyperbolic sine function can be expressed as

$$\dot{\varepsilon} = 8.67 \times 10^{11} [\sinh(0.018 \times \sigma)]^{6.326} \exp\left(-\frac{312.3 \times 10^3}{RT}\right).$$

[12]

C. Microstructure Evolution

In the hot compression process, DRX is one of the most important mechanisms for the flow softening, which can easily take place in metals and alloys with low and medium stacking fault energy, such as copper alloys, austenitic stainless steels, and γ-iron. Figure 6(a) shows an optical image of the microstructure of the Cu-2Ni-0.5Si-0.15Ag alloy deformed at 873 K (600 °C) and 1 s^{-1}. The original grains were elongated along the deformation direction, and the initial grain and twin boundaries were finely serrated (arrows in Figure 6(a)), demonstrating the occurrence of dynamic nucleation. It was suggested that dynamic nucleation takes place by bulging out of the serrated grain boundaries.[26] Moreover, grain boundaries are frequently serrated before nucleation and geometrically necessary dislocation sub-boundaries with high misorientation are developed near the interface between the new grains and the parent grains during nucleation. The characteristic of DRX is becoming more evident with the increase of deformation temperature, and then a large number of fine DRX grains appear along the initial grain boundaries, as shown in Figure 6(b). Thus, DRX is one of the main softening mechanisms, resulting in an obvious flow softening during the hot deformation processing of the Cu-2Ni-0.5Si-0.15Ag alloy.

The DRX grain size strongly depends on the deformation parameters, including temperature and strain rate. The effects of deformation temperature and strain rate on the DRX grain size can be simultaneously reflected by the *Z* parameter. Figure 7 shows optical images of the microstructure of the
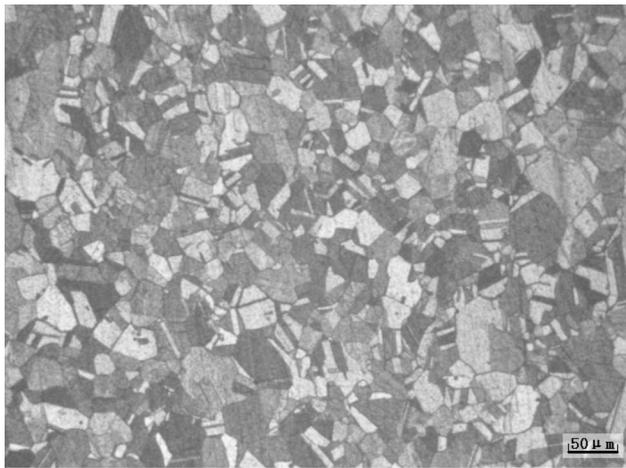

(a)

(b)

Fig. 6— Optical images of the Cu-Ni-Si-Ag alloy microstructure deformed at (a) 873 K (600 °C) and 1 s^{-1} and (b) 923 K (650 °C) and 1 s^{-1}.
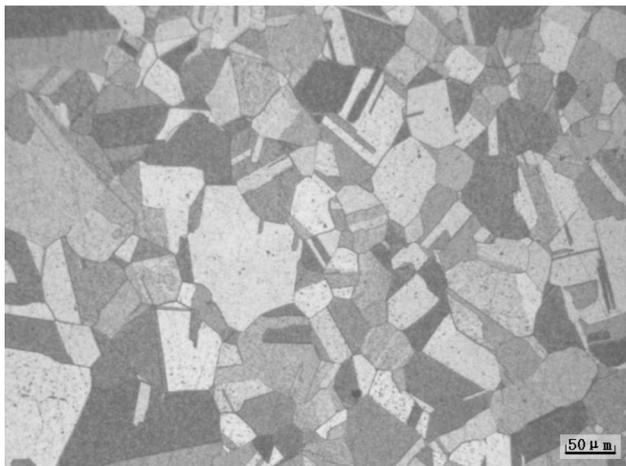
Cu-2Ni-0.5Si-0.15Ag alloy deformed at various temperatures and strain rates. The DRX grain size of the compressed sample deformed at 973 K (700 °C) and 5 s^{-1} is shown in Figure 7(a). It has finer grain size compared with the grain size of the sample deformed at 1073 K (800 °C) and 0.1 s^{-1}, as shown in Figure 7(b). Therefore, it can be concluded that the DRX behavior of the Cu-2Ni-0.5Si-0.15Ag alloy strongly depends on the deformation parameters, and lower *Z* parameter leads to more adequate DRX processing.

IV. CONCLUSIONS

Hot compression tests of the Cu-2Ni-0.5Si-0.15Ag alloy were carried out using the Gleeble-1500D thermo-simulator at 0.01 to 5 s^{-1} strain rate range and 873 K to 1073 K (600 °C to 800 °C) deformation temperature range. The addition of Ag can evidently refine the grain and optimize the hot workability of the Cu-Ni-Si alloy. Deformation at 1073 K (800 °C) and

(a)

(b)

Fig. 7— Microstructure of the Cu-2Ni-0.5Si-0.15Ag alloy deformed at (*a*) 973 K (700 °C) and 5 s^{-1} and (*b*) 1073 K (800 °C) and 0.1 s^{-1}.

5 s^{-1} strain rate is desirable and feasible for the Cu-2Ni-0.5Si-0.15Ag alloy.

(1) The flow stress of the Cu-2Ni-0.5Si-0.15Ag alloy increases with increasing the strain rate and decreasing the deformation temperature.

(2) The constitutive relationship between the peak stress, strain rate, and deformation temperature can be described by the *Z* parameter in the hyperbolic sine function with the hot deformation activation energy of 316 kJ/mol. The constitutive equation of the Cu-2Ni-0.5Si-0.15Ag alloy can be expressed as

$$\dot{\varepsilon} = 8.67 \times 10^{11} [\sinh(0.018 \times \sigma)]^{6.326} \exp\left(-\frac{312.3 \times 10^3}{RT}\right)$$

(3) The DRX mechanism is one of the most important softening mechanisms during hot deformation for the Cu-2Ni-0.5Si-0.15Ag alloy. The DRX grain size of the Cu-2Ni-0.5Si-0.15Ag alloy

strongly depends on the deformation parameters, which can be simultaneously reflected by the Zener–Hollomon parameter, *Z*. Lower *Z* parameter leads to more adequate DRX processing.

REFERENCES

1. H.T. Tran, M.H. Shirangi, X. Pang, and A.A. Volinsky: *Int. J. Fract.*, 2013, vol. 185, pp. 115–27.
2. P. Liu, B.X. Kang, X.G. Cao, J.L. Huang, B. Yen, and H.C. Gu: *Mater. Sci. Eng. A*, 1999, vol. 265, pp. 262–67.
3. S. Bera, W. Lojkowsky, and I. Manna: *Metall. Mater. Trans. A*, 2009, vol. 40A, pp. 3276–83.
4. L. Zhang, Z. Li, Q. Lei, W.T. Qiu, and H.T. Luo: *Mater. Sci. Eng. A*, 2011, vol. 528, pp. 1641–47.
5. S.W. Lee, H. Matsunaga, X. Sauvagec, and Z.J. Horita: *Mater. Charact.*, 2014, vol. 90, pp. 62–70.
6. Z. Li, Z.Y. Pan, Y.Y. Zhao, Z. Xiao, and M.P. Wang: *J. Mater. Res.*, 2009, vol. 24, pp. 2123–29.
7. Y.Q. Long, P. Liu, Y. Liu, W.M. Zhang, and J.S. Pan: *Mater. Lett.*, 2008, vol. 62, pp. 3039–42.
8. H.S. Wang, H.G. Chen, J.W. Gu, C.E. Hsu, and C.Y. Wu: *Mater. Sci. Eng. A*, 2014, vol. 619, pp. 221–27.
9. C.D. Xia, Y.L. Jia, W. Zhang, K. Zhang, Q.Y. Dong, G.Y. Xu, and M. Wang: *Mater. Des.*, 2012, vol. 39, pp. 404–09.
10. Y.L. Jia, M.P. Wang, C. Chen, Q.Y. Dong, S. Wang, and Z. Li: *J. Alloys Compd.*, 2013, vol. 557, pp. 147–51.
11. P. Hanzelka, V. Musilova, T. Kralik, and J. Vonka: *Cryogenics*, 2010, vol. 50, pp. 737–42.
12. S.G. Jia, M.S. Zheng, P. Liu, F.Z. Ren, B.H. Tian, G.S. Zhou, and H.F. Lou: *Mater. Sci. Eng. A*, 2006, vol. 419, pp. 8–11.
13. S. Suzuki, N. Shibutani, K. Mimura, M. Isshiki, and Y. Waseda: *J. Alloys Compd.*, 2006, vol. 417, pp. 116–120.
14. M.G. Corson: *Electr. World*, 1927, vol. 89, pp. 137–39.
15. C. Watanabe, S. Takeshita, and R. Monzen: *Metall. Mater. Trans. A*, 2015, vol. 46A, pp. 2469–75.
16. J.Y. Cheng, B.B. Tang, F.X. Yu, and B. Shen: *J. Alloys Compd.*, 2014, vol. 614, pp. 189–95.
17. R.A.G. Silva, A. Paganotti, A.T. Adorno, C.M.A. Santos, and T.M. Carvalho: *J. Alloys Compd.*, 2015, vol. 643, pp. S178–81.
18. Y. Liu, S. Shaoa, K.M. Liu, X.J. Yang, and D.P. Lu: *Mater. Sci. Eng. A*, 2012, vol. 531, pp. 141–46.
19. Y. Zhang, B.H. Tian, P. Liu, S.G. Jia, L. Fan, and Y. Liu: *Adv. Mater. Res.*, 2011, vols. 146–147, pp. 701–04.
20. Y.V.R.K. Prasad and K.P. Rao: *Mater. Sci. Eng. A*, 2012, vol. 487, pp. 316–27.
21. C. Zener and J.H. Hollomon: *J. Appl. Phys.*, 1946, vol. 17, pp. 69–82.
22. H. Farnoush, A. Momeni, K. Dehghani, JA Mohandesi, and H. Keshmiri: *Mater. Des.*, 2010, vol. 31, pp. 220–26.
23. A Momenia, H Arabi, A Rezaei H Badri, and S.M. Abbasi: *Mater Sci. Eng. A*, 2011, vol. 528, pp. 2158–63.
24. D.J. Li, Y.R. Feng, Z.F. Yin, F.S. Shangguan, K. Wang, Q. Liu, and F. Hu: *Mater. Des.*, 2012, vol. 34, pp. 713–18.
25. Y. Wang, W.Z. Shao, L. Zhen, and B.Y. Zhang: *Mater. Sci. Eng. A*, 2011, vol. 528, pp. 3218–27.
26. W. Gao, A. Belyakov, H. Miura, and T. Sakai: *Mater. Sci. Eng. A*, 1999, vol. 265, pp. 233–39.